Low cost fabrication of printed electronics devices through continuous wave laser-induced forward transfer

*Pol Sopeña†, Javier Arrese‡, Sergio González-Torres†, Juan Marcos Fernández-Pradas†, Albert Cirera‡, and Pere Serra†**

†Department of Applied Physics, Universitat de Barcelona, Martí i Franquès 1, 08028, Barcelona, Spain

†Institute of Nanoscience and Nanotechnology (IN2UB), Universitat de Barcelona, Joan XXIII S/N, 08028, Barcelona, Spain

‡MIND, Engineering Department: Electronics, Universitat de Barcelona, Martí i Franquès 1, 08028, Barcelona, Spain

‡Institute of Nanoscience and Nanotechnology (IN2UB), Universitat de Barcelona, Joan XXIII S/N, 08028, Barcelona, Spain

* e-mail: pserra@ub.edu

KEYWORDS: Laser-induced forward transfer, laser printing, printed electronics, paper electronics, gas sensors.

ABSTRACT

Laser induced forward transfer (LIFT) is a direct-writing technique that allows printing inks from a liquid film in a similar way to inkjet printing but with fewer limitations concerning ink viscosity and loading particle size. In this work we prove that liquid inks can be printed through LIFT by using continuous wave (CW) instead of pulsed lasers, which allows a substantial reduction in the cost of the printing system. Through the fabrication of a functional circuit on both rigid and flexible substrates (plastic and paper) we provide a proof-of-concept that demonstrates the versatility of the technique for printed electronics applications.

Inkjet printing is probably the most widespread technique for the digital manufacture of printed electronics devices.[1-3] With a long history of development in the field of the graphic arts, inkjet printing was quickly adapted to print the new materials required by the new applications with considerable success.[4] However, the technique presents constraints related with the rheological properties of the printing ink which can limit its application in some instances. Among them, the size of the particles loading the ink: a particle size of the order of $1/100^{th}$ of the output nozzle diameter usually represents the upper threshold for a printable ink (due to nozzle clogging issues)[5]. Besides, the rheology of the ink becomes fundamental and an inverse of the Ohnesorge number Z laying between 1 and 14 is required to form stable drops.[6] These issues can easily exclude several interesting materials from being printed through inkjet printing. Nanostructured materials like nanowires, nanofibers, or nanotubes, very promising in many electronic applications (smart

systems, sensors, devices, LEDs or batteries), can be hardly printed through inkjet printing without previously modifying the extreme aspect-ratios that provide them with their unique functional properties. [5,7]

Laser induced forward transfer (LIFT) has been revealed as an interesting alternative to inkjet printing in that it allows printing inks of a wide range of materials with little limitations concerning their rheological properties. The principle of operation of LIFT is rather simple (Figure 1a): a pulsed laser beam is focused on a thin film of the ink to be printed through a transparent donor substrate.[8,9] The absorption of the laser pulse at the film interface leads to the formation of a cavitation bubble which expansion results in the development of a liquid jet that propagates away the film (Figure 1b). A receiving substrate placed in front of the ink free surface intercepts the jet, which allows collecting the ejected liquid, thus leading to the formation of the sessile droplet that ultimately becomes the printed pixel.[10-13] Since the jet is generated from an unconstrained liquid, and not by means of flow through a nozzle, this sets fewer restrictions concerning the printable particle size. [14]

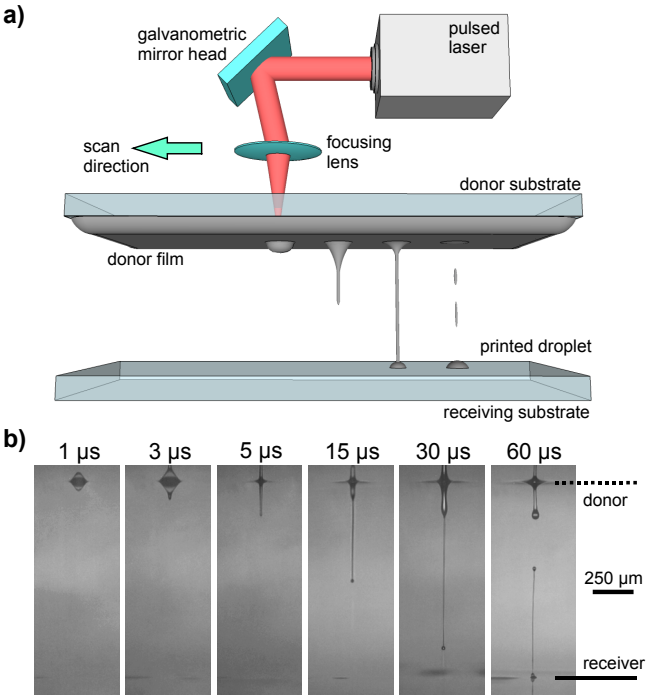

Figure 1. a) Sketch of the setup and principle of operation of pulsed LIFT. The laser beam is scanned along the donor film at a certain scan speed and repetition rate. Each laser pulse results in the formation of a long jet of ink, which contact with the receiving substrate leads to the printing of a droplet. b) Stop action movie of a printing event. In all the frames the donor film is located in the top of the image and the receiving substrate in the bottom, and the laser beam is impinging from above. The images were acquired with a time resolved microscope in shadowgraphy configuration; the acquisition delay respect to the laser pulse is indicated above each frame, and the aperture time was always 100 ns. It is observed that the jetting dynamics characteristic of pulsed LIFT results in the formation of a printed droplet through contact of the jet with the receiving substrate.

The transient character of the jetting dynamics observed in the LIFT of inks is inherent to the use of pulsed lasers, apparently a major requirement of the technique. Pulsed lasers, though, are

expensive, or at least considerably more expensive than analogous continuous wave (CW) lasers with the same output power. This issue can overshadow the interesting attributes of LIFT, and thus hinder or delay the spread of the technique in the printed electronics industry. With the aim of overcoming the drawback, here we propose carrying out the LIFT of liquid inks with CW laser radiation; this unconventional approach should allow a substantial reduction in the cost of acquisition of the laser source which in turn should impact the final production costs of the printed devices. CW lasers have already been employed for the digital transfer of materials,[15] as in the well-known laser-induced thermal imaging (LITI) technique.[16] However, in those instances transfer was always carried out from solid donor films. The CW-LIFT approach with liquid donor films that we propose here should allow broadening considerably the range of printable materials.[8] At the same time, in that transfer takes place in liquid state and with no phase change, the approach would be compatible with the use of inkjet and screen-printing inks, and therefore with all the already existing technologies in the printed electronics industry.

Upon scanning a focused CW laser beam on a donor film of a commercial ink, we prove the feasibility of CW-LIFT by means of printing continuous and stable conductive lines which can be used as interconnects in printed electronic circuits. Fast photography of liquid ejection allows us to demonstrate that material transfer proceeds through a spray mechanism apparently unrelated with the jets generated during LIFT with pulsed lasers. Finally, as a proof-of-concept for the new approach we fabricate a circuit containing a gas and a temperature sensor wherein all the printed elements have been deposited through CW-LIFT. To this aim we have used two inks of very different particle size each, and we have printed them on both rigid (glass) and flexible (polyimide and paper) substrates in order to show the versatility of the technique for printed electronics applications.

In the first printing experiments we used a commercial inkjet printing Ag ink (water-based suspension of Ag nanoparticles with an average diameter below 60 nm) as donor material and glass as receiving substrate in a typical LIFT configuration with a gap between donor and receiving substrate of 150 μm (see Supporting Information for details). With the aim of printing conductive lines we scanned the donor film with a CW-Nd:YAG laser beam (1064 nm wavelength, 100 μm beam waist diameter) following straight lines in the way presented in Figure 2a at the maximum scan speed available with our system (600 mm/s) and at different output powers. In spite that wavelengths in the visible range would be better suited for transfer attending to the radiation absorption properties of the Ag ink,[17] CW-LIFT is intended to be applied to a broad range of instances, many of which can include inks of materials with different optical properties. Therefore, the use of such an ubiquitous laser radiation as the Nd:YAG fundamental wavelength (1064 nm) seems a reasonable choice in a feasibility study like this, even if its wavelength is not the optimum one for that particular ink in terms of absorption (for a more detailed analysis of the inks absorption characteristics, please, see Supporting Information). In fact, even in instances wherein the ink is completely transparent to the laser radiation it is always possible to use an intermediate absorbing layer between the donor substrate and the donor liquid film, a strategy commonly employed in pulsed LIFT.[10,18]

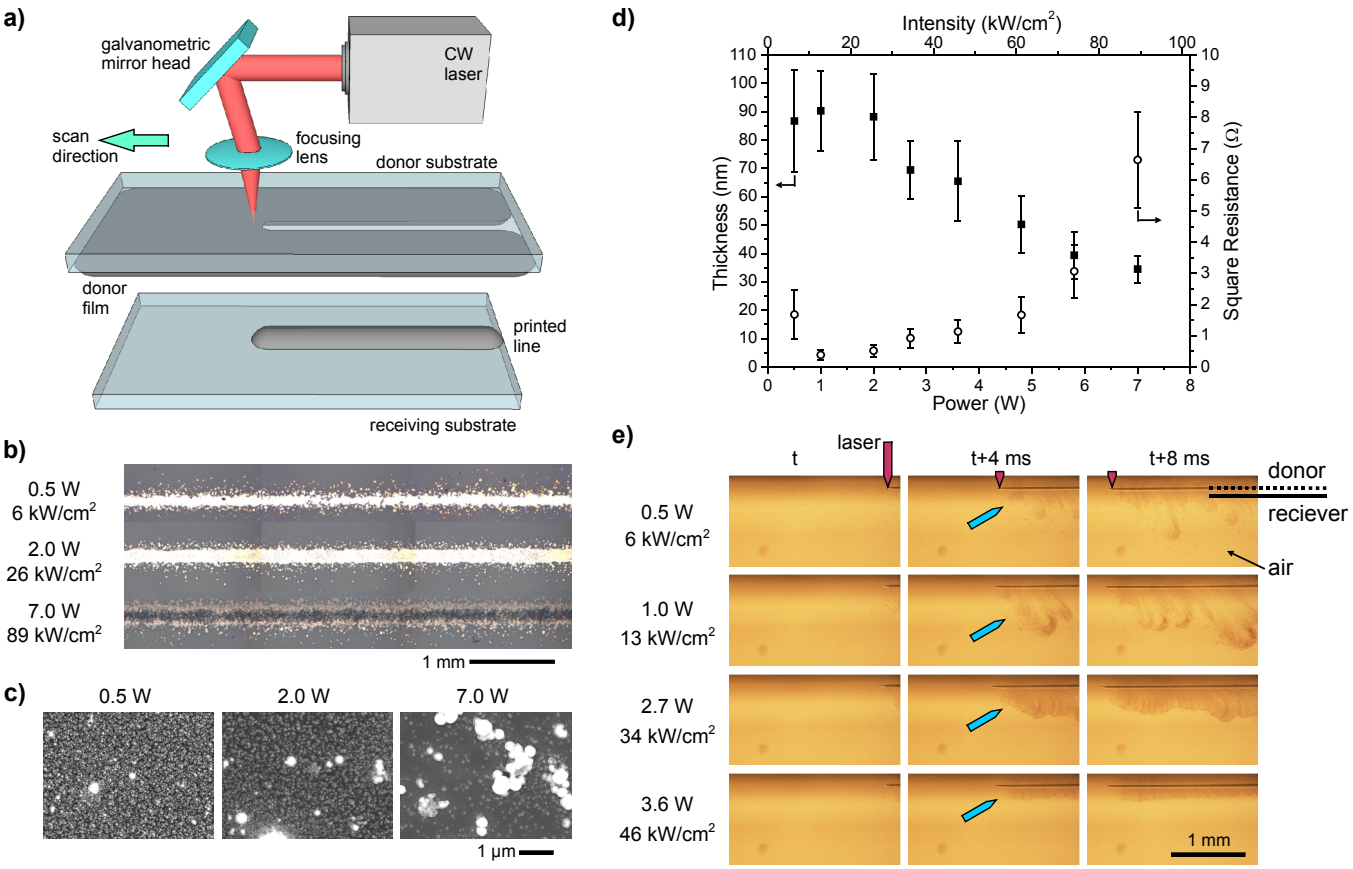

Figure 2. a) Sketch of the setup and principle of operation of CW-LIFT. The laser beam is scanned along the donor film at a certain scan speed, which results in the printing of a continuous line of ink on the receiving substrate. b) Optical microscopy images of lines of Ag ink printed through CW-LIFT on glass at a scan speed of 600 mm/s and different laser powers; the laser power and corresponding intensity (power per unit area) are displayed besides each line. The images correspond to dried ink before sintering. It is observed that continuous lines free from bulging are obtained in all cases. c) SEM images with details of the center of the printed lines. It is observed that the concentration of nanoparticles in the line decreases with laser power while the presence of large particles and aggregates increases. d) Plot of both thickness (■) and sheet resistance (○) versus laser power and intensity. The minimum sheet resistance is obtained at fairly low laser powers (1-2 W). e) Stop action movies of liquid ejection during CW-LIFT acquired through fast

photography at different laser powers and at a speed of 300 mm/s. In all the frames the donor film is located in the top of the image and there is no receiving substrate (though its eventual position is indicated in the top frames); the laser beam is impinging from above and scanning the donor film from right to left. The acquisition delay respect to an arbitrary time t is indicated above each frame, and the aperture time was always 5 μs. The blue arrow indicates the position of the ejected ink front. The real movies are provided in Supporting Information. It is observed that liquid transfer in CW-LIFT proceeds through a spraying dynamics.

Remarkably, stable continuous lines were obtained in most cases in the lines printing experiment (Figure 2b). The corresponding line widths, around 200 μm (the irregular contour represents a deviation of about 15 % around the average for 1.0-4.0 W laser powers), are perfectly acceptable in many printing applications; in fact, most commercially available printed electronics devices, as well as most realizations displayed in the literature, have similar (and even larger) minimum feature sizes.[19] Nevertheless, smaller features could be even achieved through tighter focusing of the laser beam or through improved radiation absorption in the liquid donor film (through the use of either a different laser wavelength or an intermediate absorbing layer). In spite of the presence of some spray around the edges, the lines appear to be uniformly covered with ink all along their lengths for most of the investigated laser powers; only at the highest powers (between 6 and 7 W) discontinuous deposit is observed in the center of the lines. Scanning electron microscopy (SEM) confirms that at low powers the lines are indeed uniformly coated with Ag nanoparticles (Figure 2c). In fact, at the lowest powers the particle distribution reproduces well that of the donor film. The SEM images also reveal that as the laser power is increased above 2 W, the nanoparticles concentration decreases, and larger particles (up to 0.5 μm in diameter) are found randomly

scattered onto the coating, sometimes forming aggregates. These aggregates could be attributed to nanoparticles melting and coalescence taking place during laser irradiation, being most prominent at the highest powers. Similar micron-sized ejecta have been observed during the ablation of metallic nanoparticle films with pulsed lasers.[20] The thermodynamic size effect of nanoparticles coupled to the reduced thermal conductivity of nanostructured materials can result in nanoparticle melting at substantially lower temperatures than those required for bulk metal which could account for the formation of the aggregates even at the relatively low laser powers of these experiments.[21] The different hue and reflectivity of the borders of the line at 7.0 W (Figure 2b) are probably due to the much lower density of nanoparticles, as well as to the presence of the aggregates. Finally, it is also remarkable that in spite that very long lines were printed (up to 6 cm), bulges were never found; this is noticeable, since bulging is one of the most problematic defects in printed interconnects in that they can lead to undesired short-circuits between adjacent lines.[22] Tiny droplets arising from the spray can reach distances up to about 200 μm away from the border of the line; however, they do not contribute to the line electrical properties, and therefore they do not compromise its functionality, as it will be shown later.

The plot of the average thickness of the line versus laser power (Figure 2d) displays a maximum value of around 90 nm at powers between 1 and 2 W, followed by a monotonous decrease at increasing powers (the thickness values above 5.0 W are not very significant due to the depletion of nanoparticles in the center of the lines). An equivalent plot for the sheet resistance of the lines after sintering in an oven (see Supporting Information for details on sintering conditions) shows the reversed behavior, with a minimum sheet resistance of about 0.4 Ω/□ at the same powers of 1-2 W, which corresponds to a minimum resistivity of about 3 μΩ·cm (see Supporting Information for details on the evolution of resistivity with laser power). These values are comparable to - and

even better than - those usually obtained with laser sintered metallic nanoinks.[23,24] In spite that the maximum thickness achieved is slightly lower than that obtained with inkjet printing single scans, the corresponding sheet resistance -the parameter which ultimately determines the functionality of the prints- is perfectly comparable to those characteristic of inkjet printing.[25] These results, together with the possibility of printing long continuous lines demonstrated in the previous paragraph, conclusively prove that CW-LIFT is feasible for printing conductive lines from inks to be used as interconnects in electronic circuits. Yet there is another issue that deserves attention: the optimum lines were obtained at fairly low powers in these experiments (which could be substantially reduced through tighter focusing of the laser beam). This is truly remarkable in that it means that very inexpensive lasers can be used, which positively reverts on the cost reduction initially aimed through the approach of operating in the CW regime. In fact, robust and stable CW laser diodes with powers about 1 W can be purchased for as little as a few hundred euros. Aside from cost reduction, operating with low power CW lasers presents additional advantages, like the possibility of using truly portable lasers that are easy to integrate in a production line, not to mention energy consumption and safety issues.[26]

There is an important difference between CW and conventional pulsed LIFT yet to be considered, the transfer process. The jetting dynamics of pulsed LIFT (Figure 1b) is hardly compatible with the continuous nature of the new approach. So, how does liquid transfer proceed in CW-LIFT? In order to answer this question we carried out fast photography of ink ejection in the absence of any receiving substrate at different laser powers. A slower speed (300 mm/s) than that used in the printing experiments was set in order to acquire a number of frames high enough to properly reproduce the movie of the process with a magnification allowing to visualize the ejected liquid under all the analyzed conditions. The selection of frames presented in Figure 2e

reveals that the laser beam atomizes the liquid as it scans the donor film and projects it towards the receiving substrate as a spray, a transfer dynamics completely different from that of pulsed LIFT (the complete movies are provided in Supporting Information). The broad spray angle does not represent a critical problem for printing since the typical gap between donor and receiver in LIFT is small enough to allow ink collection before there is too much spread on the receiving substrate. In fact, the observed dynamics allows understanding the tiny sprayed droplets around the edges of the printed lines described before. The unexpected spray dynamics could be attributed to the longer irradiation times compared to pulsed LIFT (in fact, the laser peak intensities during the CW-LIFT of liquids are more than four orders of magnitude smaller than those of conventional pulsed LIFT). In contrast with the pulsed case, wherein a single cavitation bubble generated at the solid-liquid interface was responsible for jetting, now practically the entire thickness of the irradiated film is heated by the laser beam, and at a much slower rate. We have estimated a heat penetration depth of around 30 μm and a total irradiation time of 340 μs for a scanning speed of 300 mm/s, an irradiation time several orders of magnitude above the few nanoseconds characteristic of pulsed LIFT. Since the estimated time required for boiling inception of the entire liquid film (t_B=8 μs) is substantially lower than that, we can consistently assume the onset of pool boiling in the irradiated portion of the ink (the consistency of this hypothesis with the characteristic length and time scales of the process is discussed in detail in Supporting Information). The splash originated by the bursting tiny bubbles during pool boiling would account for the observed atomization of the liquid, and therefore for the spraying dynamics. Furthermore, the images also reveal that the intensity of the spray peaks at 1-2 W to later decrease at higher powers, which correlates well with the line thickness evolution observed in Figure 2d. This can also be correlated with the dark band observed in the center of the printed lines at high powers (Figure 2b). In

experiments of laser sintering of metallic nanoparticle films it is observed the displacement of ink towards the edges of the laser scanned lines due to thermocapillary flow induced by laser heating.[17] That flow would be responsible for the depletion of material along the center of the irradiated lines, and it would therefore account for the decrease in the intensity of the spray observed above 1.0 W. A final consequence of this would be the absence of deposited material observed in the central part of the lines printed at the highest powers (Figure 2b).

In order to provide a convincing proof-of-concept for the feasibility of the technique in printed electronics applications, we fabricated a functional device through the CW-LIFT of liquid inks: a gas and a temperature sensing circuit. Aside from the environmental interest of both magnitudes, temperature affects the response of most gas sensors, with much work devoted to this with the proposed gas sensing material.[27] Furthermore, sensing is an important sector in the field of printed electronics, so that with our choice we are aiming at an application with broad scope and significant potential impact. In fact, this is one of the reasons why a considerable variety of sensors have also been fabricated through conventional pulsed-LIFT.[28,29] We first printed the same Ag ink used in the previous experiments at a laser power of 1 W and a scan speed of 600 mm/s in order to produce a series of narrow interdigitated electrodes, as well as additional wider interconnects, these last ones generated by printing parallel overlapping lines (Figure 3a). The electrical characterization of the printed elements showed that the interdigitated electrodes are in open circuit condition, which proves that the residual spray around the edges of the printed lines does not compromise the functionality of the electrodes. We then printed in identical irradiation conditions a square pad of carbon nanofibers (CNF), the gas sensing material, from an aqueous suspension onto the interdigitated electrodes, and assembled a surface mount thermistor (the temperature sensing element) to the printed interconnects alongside four contacts for measurements (Figure 3b). CNFs

are a promising material in gas sensing applications thanks to their high sensitivity [27] as well as to their elongated graphene-like structure, which allows devising strategies for self-heating in the nanoscale. On the other hand, the inclusion of the thermistor allows proving the compatibility of the stripes printed through CW-LIFT with surface-mount technology. The entire pattern was fabricated onto three different substrates: glass (Figure 3a, b), polyimide (Figure 3c) and paper (Figure 3d). Glass is a quite standard non-porous, flat and rigid substrate, especially suited to test the performance of the printing technique under ideal conditions. The other two substrates are more technologically relevant, and should help to test the potential of CW-LIFT in areas with such a high impact as flexible plastic and paper electronics.

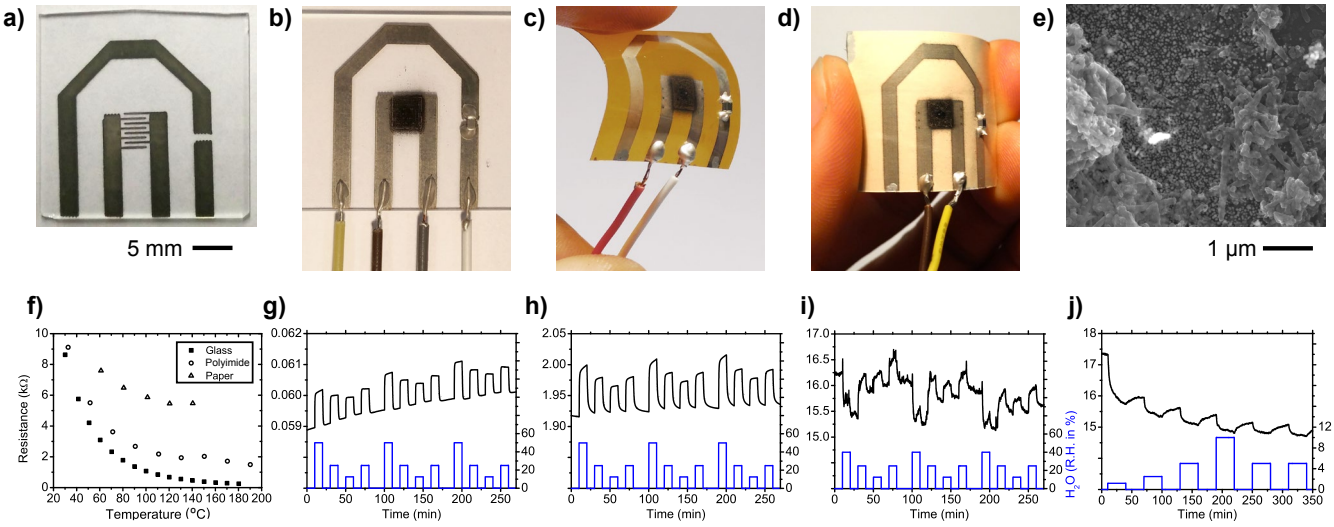

Figure 3. Gas and temperature sensor printed through CW-LIFT. a) Ag ink electrodes printed on glass at a laser power of 1 W and a scan speed of 600 mm/s; the image corresponds to sintered electrodes. Time to print the entire set: 2 s. b) Finished sensor displaying the gas sensing pad (CNFs printed through CW-LIFT at the same conditions onto the area delimited by the interdigitated electrodes), the surface mount thermistor soldered to the outer set of electrodes, and the contacts for measurements. c) The same sensor printed on polyimide. d) The same sensor

printed on paper. e) SEM image of a detail of the gas sensing pad, which displays the relatively large CNFs on a background of Ag tiny nanoparticles. f) Resistance versus temperature curve of the surface mount thermistor corresponding to the sensor printed on glass (■), polyimide (○) and paper (△). Dynamic resistance of the gas sensor to humidity for the device printed on g) glass, h) polyimide, i) paper and j) to NO_2 for the device printed on paper. These plots prove the functionality of the printed sensors.

The complete set of Ag electrodes (Figure 3a), around 2 cm × 2 cm in size, was printed in a single scan in only two seconds, a time short enough to overcome any potential solvent drying issues during printing. The CNF pad, on the other hand, is a square of 4 mm × 4 mm, which also took around two seconds to print; in spite that the pad is much smaller than the electrodes, up to 10 scans were required to uniformly cover its entire area, thus the longer time required to print it. The successful printing of the CNF pad is remarkable. First, CNFs are elongated structures with diameters below 100 nm but above 1 μm long. Such interesting aspect-ratio lays clearly beyond the limits of common inkjet nozzles. In this regard, Figure 3e illustrates very well the capability of CW-LIFT to print extremely different particle sizes: the large CNFs lay on a bed of tiny Ag nanoparticles in the interdigitated electrodes. Second, no complex formulation was required for the CNF ink (the CNF were simply suspended in water and the resulting liquid suspension was printed immediately thereafter) and therefore no chemical residual is expected once the solvent is evaporated after printing, an important issue for a gas sensor. This represents another significant advantage of LIFT in terms of simplicity, cost reduction and chemical purity: many materials can be printed without the need for complex ink formulations, a process which is usually time consuming, complicated and expensive.[1] It is also worth noting that both materials, Ag

nanoparticles and CNFs, were printed with good definition not only on glass, but also onto the more challenging polyimide and paper substrates (Figure 3c, d). This is especially remarkable for paper, for which up to ten scans were required for the Ag electrodes due to its relatively high porosity (in the case of polyimide a single scan was enough).

In order to determine the response of the sensors both to temperature and to the presence of gases, we tested the entire set following the procedures detailed in the Experimental section of Supporting Information. The surface mounted thermistor exhibits a negative temperature coefficient when exposed to a hotplate (Figure 3f). An ideal behavior is observed in the sensor deposited on glass, in good agreement with the specifications of the device. A similar behavior is obtained with the sensor printed on polyimide, though with a higher contact resistance. Worse results are obtained in the case of paper, where heat transfer issues and chemical reactions could arise. Concerning the CNFs response to gases, it was first investigated before water vapor for the three different substrates with unheated CNFs (Figure 3g-i). In the case of glass, the CNFs resistance increases with the water pulses as expected, showing good stability within a sequence of pulses. However, the baseline increases along the different sequences of pulses. In the case of polyimide a higher resistance is observed, as well as a slightly longer response/recovery time, but improved baseline. Nevertheless, both responses are in good agreement with previous results.[27,30] In the case of the sensor on paper, the hydrophilicity of this substrate seems to induce a backfilling process when recovering the sensor with synthetic air that results in rather inconsistent measurements. Paper does not seem, therefore, an adequate substrate for water vapor sensing. In order to test the sensor with a more suited gas, we chose NO_2, which should be free from backfilling issues. In this case the sensor response is similar to that previously obtained for that gas on a polyimide [27] and on a ceramic substrate.[30] It should be noted, nonetheless, that the sensing

material is not heated in the present case. A simple heating at 40-60ºC would stabilize the baseline and improve the response/recovery times, eventually providing even better results. Alternatively, an advanced self-heating strategy of the CNFs at the nanoscale could be applied with the same aim.[30]

In conclusion, we have proved that CW-LIFT allows the digital printing of functional inks from liquid donor films at high speed and with few restrictions concerning the size of the particles loading the ink. As with conventional pulsed LIFT, in some instances this approach can present significant advantages over other printing techniques, like inkjet printing, in that it allows broadening the range of materials which can be digitally printed; nanostructured materials, for example, can be successfully transferred without altering the high aspect ratios that confer their unique functional properties. But it also represents a substantial advantage over pulsed LIFT itself, since the use of CW instead of pulsed lasers can result in a remarkable cost reduction in the setting up of the printing unit, even more considering that we have demonstrated that optimum results can be obtained with relatively low powers, and therefore with very inexpensive lasers. Finally, through the fabrication of an operative gas and temperature sensing circuit we have provided a valuable proof-of-concept of CW-LIFT in at least such a relevant printed electronics application as sensors manufacturing, and have shown that the technology is compatible with the use of flexible plastic and paper substrates.

ASSOCIATED CONTENT

Supporting information

The Supporting Information is available free of charge on the ACS Publications website.

Additional experimental details and calculation of the pool boiling hypothesis (PDF)

Movie showing the transfer dynamics (MP4)

AUTHOR INFORMATION

Corresponding Author

Pere Serra.

E-mail: pserra@ub.edu

Author Contributions

The manuscript was written through equal contributions of all authors. All authors have given approval to the final version of the manuscript.

Notes

The authors declare no competing financial interest.

ACKNOWLEDGEMENT

This work was funded by MINECO of the Spanish Government (Projects TEC2014-54544-C2-1-P and TEC2015-72425-EXP) and also by Fondo Europeo de Desarrollo Regional (FEDER). The authors would like to thank E. Lendínez for his help in the acquisition of the time resolved images corresponding to pulsed LIFT. A. Cirera acknowledges support from the 2015 edition of BBVA Foundation Grants for Researchers and Cultural Creators.

REFERENCES

(1) Vescio, G.; López-Vidrier, J.; Leghrib, R.; Cornet, A.; Cirera, A. Flexible Inkjet Printed High-K HfO_2-Based MIM Capacitors. *J. Mater. Chem. C* **2016**, *4*, 1804-1812.

(2) Ma, S.; Ribeiro, F.; Powell, K.; Lutian, J.; Møller, C.; Large, T.; Holbery, J. Fabrication of Novel Transparent Touch Sensing Device Via Drop-Ondemand Inkjet Printing Technique. *ACS Appl. Mater. Interfaces* **2015**, *7*, 21628-21633.

(3) Wang, Y.; Guo, H.; Chen, J.; Sowade, E.; Wang, Y.; Liang, K.; Marcus, K.; Baumann, R.R.; Feng, Z. Paper-Based Inkjet-Printed Flexible Electronic Circuits. *ACS Appl. Mater. Interfaces* **2016**, *8*, 26112-26118.

(4) Liu, M.; Wang, J.; He, M.; Wang, L.; Li, F.; Jiang, L.; Song, Y. Inkjet Printing Controllable Footprint Lines by Regulating the Dynamic Wettability of Coalescing Ink Droplets. *ACS Appl. Mater. Interfaces* **2014**, *6*, 13344-13348.

(5) Bonaccorso, F.; Bartolotta, A.; Coleman, J.N.; Backes, C. 2D-Crystal-Based Functional Inks. *Adv. Mater.* **2016**, *28*, 6136-6166.

(6) Osch, T.H.J.; Perelaer, J.; Laat, A.W.M.; Schubert, U.S. Inkjet Printing of Narrow Conductive Tracks on Untreated Polymeric Substrates. *Adv. Mater.* **2008**, *20*, 343-345.

(6) Finn, D.J.; Lotya, M.; Coleman, J.N. Inkjet Printing of Silver Nanowire Networks. *ACS Appl. Mater. Interfaces* **2015**, *7*, 9254-9261.

(8) Arnold, C.B.; Serra, P.; Piqué, A. Laser Direct-Write Techniques for Printing of Complex Materials. *MRS Bull.* **2007**, *32*, 23-31.

(9) Delaporte, P.; Alloncle, A.P. Laser-Induced Forward Transfer: a High Resolution Additive Manufacturing Technology. *Opt. Laser Technol.* **2016**, *78*, 33-41.

(10) Brown, M.S.; Kattamis, N.T.; Arnold, C.B. Time-Resolved Dynamics of Laser-Induced Micro-Jets from Thin Liquid Films. *Microfluid. Nanofluid.* **2011**, *11*, 199-207.

(11) Mathews, S.A.; Auyeung, R.C.Y.; Kim, H.; Charipar, N.A.; Piqué, A. High-Speed Video Study of Laser-Induced Forward Transfer of Silver Nano-Suspensions. *J. Appl. Phys.* **2013**, *114*, 064910.

(12) Patrascioiu, A.; Fernández-Pradas, J.M.; Palla-Papavlu, A.; Morenza, J.L.; Serra, P. Laser-Generated Liquid Microjets: Correlation Between Bubble Dynamics and Liquid Ejection. *Microfluid. Nanofluid.*, **2014**, *16,* 55-63.

(13) Florian, C.; Piazza, S.; Diaspro, A.; Serra, P.; Duocastella, M. Direct Laser Printing of Tailored Polymeric Microlenses. *ACS Appl. Mater. Interfaces* **2016**, *8*, 17028-17032.

(14) Papazoglou, S.; Tsouti, V.; Chatzandroulis, S.; Zergioti, I. Direct Laser Printing of Graphene Oxide for Resistive Chemosensors. *Opt. Laser Technol.* **2016**, *82*, 163-169.

(15) Yung, W.K.C.; Sun, B.; Meng, Z.; Huang, J.; Jin, Y.; Choy, H.S.; Cai, Z.; Li, G.; Ho, C.L.; Yang, J.; Wong, W.Y. Additive and Photochemical Manufacturing of Copper. *Sci. Rep.* **2016**, *6*, 39584-1 - 39584-9.

(16) Lee, J.Y.; Lee, S.T. Laser-Induced Thermal Imaging of Polymer Light-Emitting Materials on Poly(3,4-Ethylenedioxythiophene): Silane Hole-Transport Layer. *Adv. Mat.* **2004**, *16*, 51-54.

(17) Chung, J.; Ko, S.H.; Bieri, N.R.; Grigoropoulos, C.P.; Poulikakos, D. Conductor Microstructures by Laser Curing of Printed Gold Nanoparticle Ink. *Appl. Phys. Lett.* **2004**, *84*, 801-803.

(18) Ko, S.H.; Pan, H.; Ryu, S.G.; Misra, N.; Grigoropoulos, C.P.; Park, H.K. Nanomaterial Enabled Laser Transfer for Organic Light Emitting Material Direct Writing. *Appl. Phys. Lett.* **2008**, *93*, 151110.

(19) Venkata Krishna Rao, R.; Venkata Abhinav, K.; Karthik, P.S.; Prakash Singh, S. Conductive Silver Inks and Their Applications in Printed and Flexible Electronics. *RSC Adv.* **2015**, *5*, 77760-77790.

(20) Ko, S.H.; Choi, Y.; Hwang, D.J.; Grigoropoulos, C.P. Nanosecond Laser Ablation of Gold Nanoparticle Films. *Appl. Phys. Lett.* **2006**, *89*, 141126.

(21) Kim, W.; Zide, J.; Gossard, A.; Klenov, D.; Stemmer, S.; Shakouri, A.; Majumdar, A. Thermal Conductivity Reduction and Thermoelectric Figure of Merit Increase by Embedding Nanoparticles in Crystalline Semiconductors. *Phys. Rev. Lett.* **2006**, *96*, 045901.

(22) Florian, C.; Caballero-Lucas, F.; Fernández-Pradas, J.M.; Artigas, R.; Ogier, S.; Karnakis, D.; Serra, P. Conductive Silver Ink Printing through the Laser-Induced Forward Transfer Technique. *Appl. Surf. Sci.* **2015**, *36*, 304-308.

(23) An, K.; Hong, S.; Han, S.; Lee, H.; Yeo, J.; Ko, S.H. Selective Sintering of Metal Nanoparticle Ink for Maskless Fabrication of an Electrode Micropattern using a Spatially Modulated Laser Beam by a Digital Micromirror Device. *ACS Appl. Mater. Interfaces* **2014**, *6*, 2786-2790.

(24) Kwon, J.; Cho, H.; Eom, H.; Lee, H.; Suh, Y.D.; Moon, H.; Shin, J.; Hong, S.; Ko, S.H. Low-Temperature Oxidation-Free Selective Laser Sintering of Cu Nanoparticle Paste on a Polymer Substrate for the Flexible Touch Panel Applications. *ACS Appl. Mater. Interfaces* **2016**, *8*, 11575-11582.

(25) Gysling, H.J. Nanoinks in Inkjet Metallization - Evolution of Simple Additive-Type Metal Patterning. *Curr. Opin. Colloid Interface Sci.* **2014**, *19*, 155-162.

(26) Berrospe-Rodriguez, C.; Visser, C.W.; Schlautmann, S.; Ramos-Garcia, R.; Fernandez Rivas, D. Continuous-Wave Laser Generated Jets for Needle Free Applications. *Biomicrofluidics* **2016**, *10*, 014104.

(27) Claramunt, S.; Monereo, O.; Boix, M.; Leghrib, R.; Prades, J.D.; Cornet, A.; Merino, P.; Merino, C.; Cirera, A. Flexible Gas Sensor Array with an Embedded Heater Based on Metal Decorated Carbon Nanofibres. *Sens. Actuators B* **2013**, *187*, 401-406.

(28) Palla-Papavlu, A.; Mattle, T.; Temmel, S.; Lehmann, U.; Hintennach, A.; Grisel, A.; Wokaun, A.; Lippert, T. Highly Sensitive SnO_2 Sensor via Reactive Laser-Induced Forward Transfer. *Sci. Rep.* **2016**, *6*, 25144-1 - 25144-9.

(29) Luo, J.; Pohl, R.; Qi, L.; Römer, G-W.; Sun, C.; Lohse, D.; Visser, C.W. Printing Functional 3D Microdevices by Laser-Induced Forward Transfer. *Small* **2017**, *13*, 1602553-1 - 1602553-5.

(30) Monereo, O.; Prades, J.D.; Cirera, A. Self-Heating Effects in Large Arrangements of Randomly Oriented Carbon Nanofibers: Application to Gas Sensors. *Sens. Actuators B* **2015**, *211*, 489-497.

TABLE OF CONTENTS

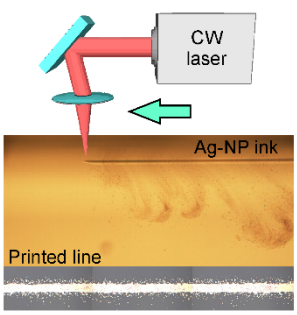

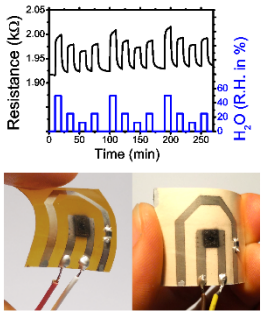

SUPPORTING INFORMATION

Low cost fabrication of printed electronics devices through continuous wave laser-induced forward transfer

*Pol Sopeña[†], Javier Arrese[‡], Sergio González-Torres[†], Juan Marcos Fernández-Pradas[†], Albert Cirera[‡], and Pere Serra[†]**

[†]Department of Applied Physics, Universitat de Barcelona, Martí i Franquès 1, 08028, Barcelona, Spain

[†]Institute of Nanoscience and Nanotechnology (IN2UB), Universitat de Barcelona, Joan XXIII S/N, 08028, Barcelona, Spain

[‡]MIND, Engineering Department: Electronics, Universitat de Barcelona, Martí i Franquès 1, 08028, Barcelona, Spain

[‡]Institute of Nanoscience and Nanotechnology (IN2UB), Universitat de Barcelona, Joan XXIII S/N, 08028, Barcelona, Spain

* e-mail: pserra@ub.edu

Experimental details

Laser: A Nd:YAG laser (Baasel Lasertech, LBI-6000), with a wavelength of 1064 nm, a nearly Gaussian beam intensity distribution and a maximum power of 50 W, was used in all the printing experiments operating in CW mode. The laser was furnished with a galvanometric mirrors head that allowed scanning the beam following predefined patterns. After the mirrors, an f-theta lens with a focal length of 100 mm focused the laser beam onto the sample, which resulted in a beam waist diameter in the focal plane of about 100 μm. The laser beam scan speed in the focal plane could be tuned from 1 to 600 mm/s.

Materials: Two different inks were used for printing. The first one was a commercial Ag nanoparticle ink (Metalon® JS-B25HV) typically used for inkjet printing. It is an aqueous dispersion of Ag nanoparticles smaller than 60 nm, with a solid content of around 25 wt. %, a density of 1.3 g/cm³ and a viscosity of 8 mPa·s. This ink was used for the morphological study of the printed lines, the time resolved characterization of the transfer process and the fabrication of the electrodes for the sensors. The second ink was prepared by simply suspending CNFs in distilled water, with a resulting concentration of 20 mg/mL. The CNFs, provided by Grupo Antolin, have a helicoidally graphitic stacked cup structure, with a presence of 6 % of Ni, a diameter of 20-80 nm, a length ranging from several microns up to 30 μm, and a specific surface of 150-200 m^2/cm^3 (Brunauer–Emmett–Teller, N_2).[1] The gas sensing pads were printed with this CNF ink. The radiation absorption properties of both Ag and CNF inks were measured with a Perkin Elmer Lambda 950 spectrophotometer in the 400-1200 nm range. Three different materials were used as receiving substrates. The first one was glass (Deltalab microscope slides, 76 mm × 26 mm × 1 mm), used in the morphological study of the printed lines and also in the preparation of the sensors. The sensors were also printed on polyimide (DuPont Kapton® HN, foils 75 μm thick) and paper

(Arjowiggins, Powercoat HD 230, 220 g/m^2, foils 220 μm thick). The donor films were prepared by spreading the inks by means of a blade on a glass slide like the ones described above. Volumes of 40 μL of Ag ink and of 120 μL of CNF ink were pipetted and deposited along a line transverse to the respective glass slides and spread in the same way as that shown in the video of Ref. [2] (in our case the inks are not left to dry before transfer). The resulting thicknesses (estimated through weight measurements) of the donor films were 30 μm for the Ag ink and 100 μm for the CNF ink. A gap of 150 μm between donor and receiving substrates was kept through spacers in all the CW-LIFT experiments. During the printing process the receptor substrates were held at a temperature of 75 °C in order to promote the fast evaporation of the volatile solvents aiming to a minimization of ink spreading, as well as to a reduction of the Marangoni effect due to the fixation of the particles to the substrate. The Ag ink features printed on glass and polyimide were sintered in an oven at 200 ºC for 1 hour, while those printed on paper were sintered at 170 ºC the same amount of time. The CNF ink was simply let dry after printing at room temperature, without any sintering treatment. A surface-mounted negative temperature coefficient thermistor, component size 0805 (2.0 mm × 1.25 mm), was assembled onto the printed silver pads. Silver epoxy (Chemtronics, CircuitWorks Conductive Epoxy CW2400) was used as electrical connecting material.

Characterization of the transfer process: The morphological characterization of all the samples was carried out through optical microscopy (Carl Zeiss, model AX10 Imager.A1), confocal microscopy (Sensofar PLμ 2300), and SEM (JEOL J-7100). The ink transfer dynamics was analyzed with a fast photography setup. A 1000 frames per second camera (AOS Technologies AG, model S-PRI F1) coupled to a 10x microscope objective with a numerical aperture of 0.28 was placed at grazing incidence respect to the donor substrate so that it was possible to record liquid ejection as the laser beam scanned the donor film. The images acquisition setup was

illuminated by means of a 150 W halogen lamp (ThorLabs Inc, model OSL1-EC) in a typical shadowgraphy configuration.

Characterization of the printed sensors: The thermistors were tested by using a hot plate chuck. The gas sensors where tested in a customized small-volume (15 ml) gas test chamber, where they were submitted to gas pulses with a flow of 200 ml/min in all the experiments. Two different gases were tested: water vapor for all the sensors, and NO_2 only for those printed on paper. In the case of water vapor, the desired humidity level was set by mixing saturated (by bubbling) and dry synthetic air through mass flow controllers. A sequence of four different concentrations was repeated four times for each sensor. In the case of NO_2 the measurement was done with no humidity. Its concentration was set also by mixing synthetic air and NO_2 through mass flow controllers. The electrical measurements during the gas test experiments were performed with a Keithley 2401 sourcemeter unit. The sensors were not heated during the experiments.

Our work follows the quality assessment (Q.A.) rules of the Q.A. office of the University of Barcelona as described in Ref. [3].

Radiation absorption properties of the inks

The measured spectral absorptance (percentage of absorption) of liquid films of Ag and CNF inks is presented in Figure S1a. The high solid content of both inks made impossible to detect any transmitted radiation in films with a thickness similar to that of the donor films used in CW-LIFT experiments; they were completely opaque to our spectrophotometer detector practically all along the analyzed spectrum. Therefore, we used substantially thinner films for the measurements. In the case of Ag ink, in spite that the maximum absorption takes place in the visible region (with a strong

contribution due to nanoparticle plasmonic resonance), there is no negligible absorption at the laser wavelength (1064 nm), an absorption which will become more important as the film thickness is increased. On the other hand, the CNF ink presents a flat response to all analyzed wavelengths, with high absorption levels for the measured film.

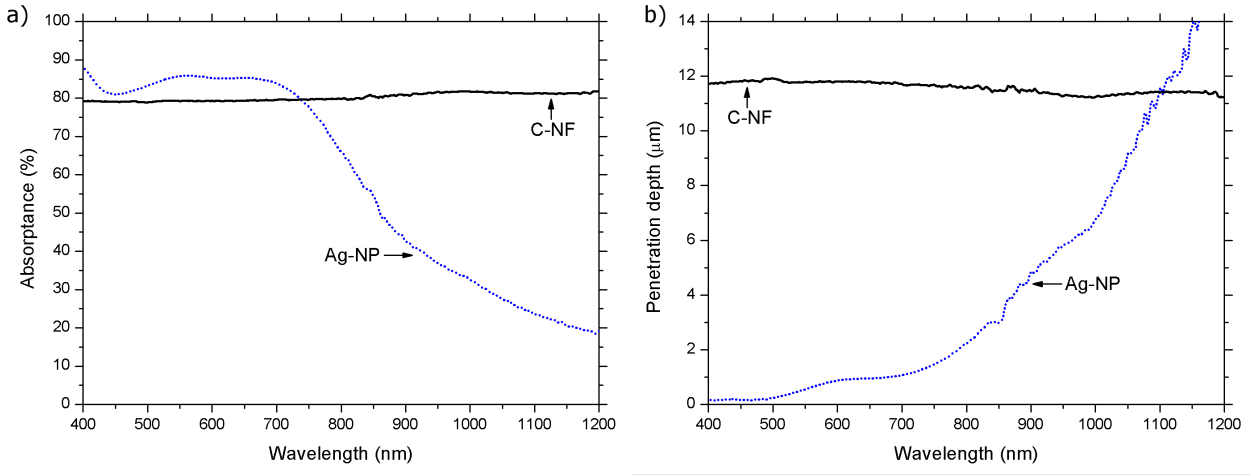

Figure S1. a) Spectral absorptance of a Ag ink liquid film 1.5 μm thick (blue dotted line) and a CNF ink liquid film 20 μm thick (black straight line). b) Dependence with wavelength of the optical penetration of the previous inks. The penetration depth of the 1064 nm laser radiation is 9 μm for the Ag ink and 11 μm for the CNF ink. In both cases the optical penetration depth is smaller than the respective donor films used in the CW-LIFT experiments.

The relevant parameter that ultimately determines the response of the liquid films to the laser radiation is the optical penetration depth at the 1064 nm wavelength. In Figure S1b we present for both Ag and CNF inks the spectral evolution of that parameter obtained from the absorptance measurements. According to these results, the optical penetration depth for the Ag ink is about 9 μm and 11 μm for the CNF ink. These depths, both substantially smaller than the respective

donor film thicknesses in the CW-LIFT experiments, indicate that all the laser radiation is absorbed within the liquid.

SEM images of printed patterns

Larger versions of the SEM images displayed in Figures 2c and 3e of the article.

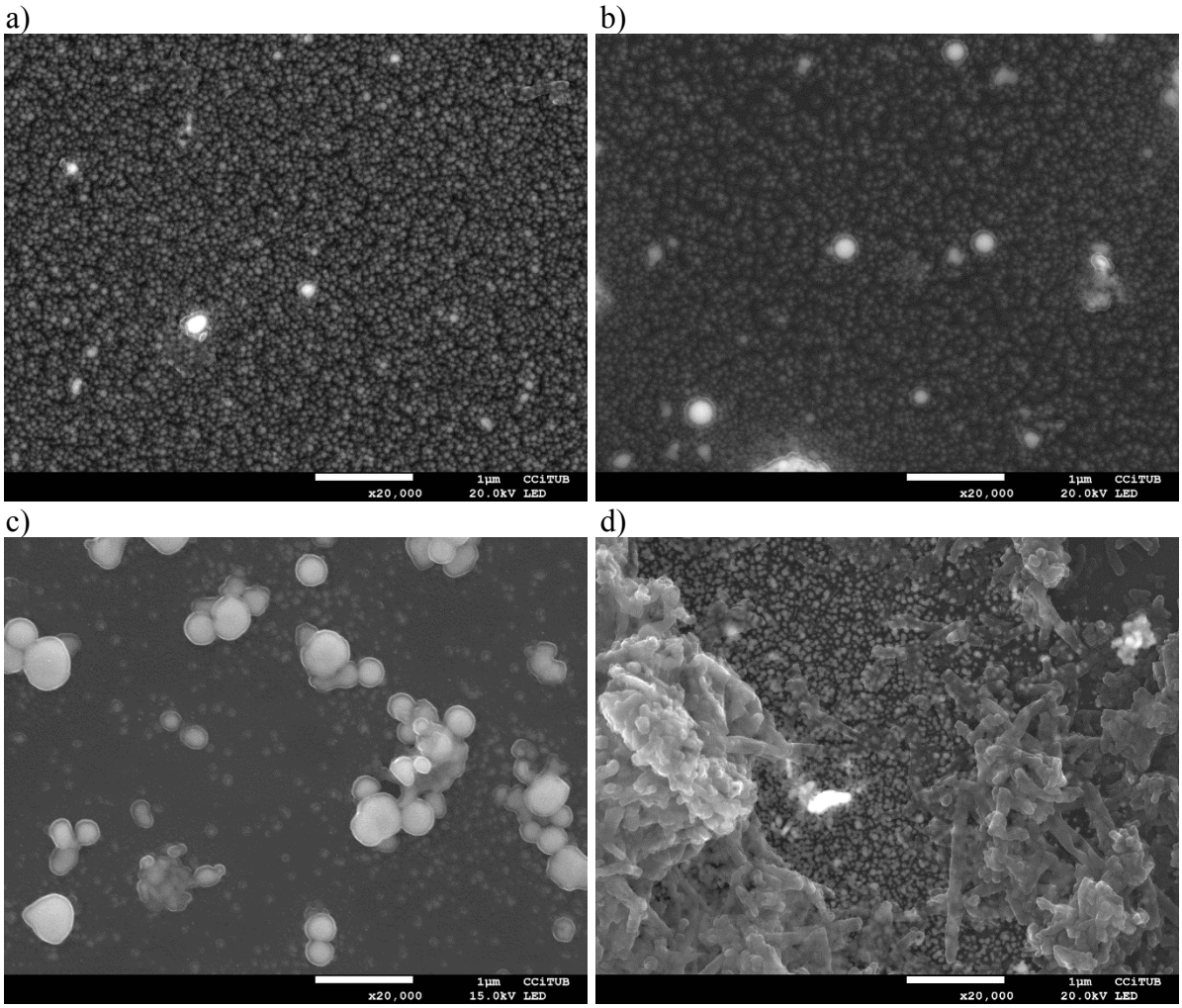

Figure S2. SEM images of the center of the silver nanoparticle lines printed at different laser pulse powers: a) 0.5, b) 2.0 and c) 7.0 W. d) Detail of carbon nanofibers on top of the silver nanoparticles corresponding to the interdigitated electrodes.

Dependence of resistivity versus laser power and intensity

The dependence of resistivity with both laser power and intensity is provided in Figure S3.

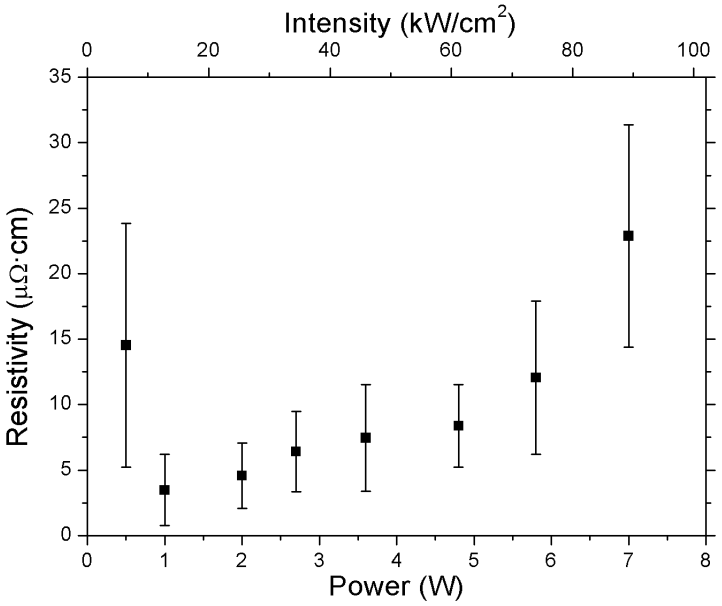

Figure S3. Plot of line resistivity versus laser power and intensity. The minimum resistivity value, around 3 μΩ·cm, is obtained at fairly low laser powers (1-2 W).

It is possible to provide a plausible explanation for this behavior based on the observed morphological characteristics of the printed lines. The high resistivity obtained at a laser power of 0.5 W can be attributed to the extremely irregular contour of the line, that can result in very small local widths at random positions within the line; 0.5 W is a power very close to the transfer threshold, so that any tiny instability in the laser can locally affect the amount of deposited material (thus the large error bar for this power, otherwise not adequate for printing). The further slow and monotonous increase in resistivity between 1 and 5 W correlates well with the observed decrease in the concentration of nanoparticles with laser power (Figures 2c and S2); a less compact line

presents a higher resistivity. Between 6 and 7 W the concentration of nanoparticles decreases dramatically in the center of the lines, which corresponds well with the sudden increase observed in resistivity (as for 0.5 W, these high laser powers are not adequate for printing).

Calculation

We have attributed the unexpected spray dynamics observed in the movies of ink transfer during CW-LIFT to a pool boiling phenomenon in the portion of the donor film irradiated by the laser beam. The longer irradiation times compared to pulsed LIFT would allow the relatively slow heating of the irradiated area, so that heat would diffuse deep inside the ink instead of being confined in a small region around the solid-liquid interface, as when short pulse lasers are used. This would lead to the formation of a myriad of tiny droplets due to the boiling of a significant fraction of the total donor film thickness, which burst would result in the observed spray.

The rigorous verification of this thesis would require solving a rather complex problem which is completely out of the scope of this work. However, we think that it is at least possible to validate its consistency through the assessment of certain characteristic lengths and times of the process. Such assessment will require some bold assumptions and rough estimates; in consequence, only the order of magnitude of the obtained results must be considered in the analysis. This is, nevertheless, enough for our purpose.

Assuming that the intensity distribution of the laser beam is uniform, for a laser beam with a diameter $D=100\ \mu m$ scanned at a speed $v=300\ mm/s$ the irradiation time t_i for any portion of the scanned line is:

$$t_i = \frac{D}{v} \sim 340\ \mu s \qquad (1)$$

This irradiation time is much longer than the ones typical of pulsed LIFT experiments, which correspond to the laser pulse duration, normally of the order of ns or less.

On the other hand, from the radiation absorption measurements presented above we have found the optical penetration depth l_{opt} in Ag ink for 1064 nm radiation to be around 9 μm.

We can estimate the thermal penetration depth l_{th} for the obtained irradiation time t_i as (all the values corresponding to properties of the materials used in the calculations are provided in Table S1):

$$l_{th} \sim \sqrt{\frac{2kt_i}{\rho_m c_p}} \sim 30\ \mu m \qquad (2)$$

where k is the thermal conductivity of the Ag ink, ρ_m its mass density and c_p its specific heat capacity.

Material	Property	Symbol	Value
Ink	Electrical resistivity	ρ_e	5×10^{-4} Ω·m
	Mass density	ρ_m	1.3×10^{3} kg/m^3
	Specific heat	c_p	245 J/(kg·K)
Water	Thermal conductivity	κ	0.591 W/(m·K)
	Surface tension (373 K)	γ	0.059 N/m
	Latent heat	L	2.26×10^{6} J/kg
	Density of vapor	ρ_v	1 kg/m^3
	Density of water	ρ_L	10^{3} kg/m^3

Table S1: Parameters used in the calculations.

Since $l_{th} > l_{opt}$, it is clear that the penetration depth of the energy deposited by the laser beam will be determined by l_{th} instead of l_{opt}, and that that energy will diffuse deep inside the donor film, affecting all of its thickness.

We should now estimate the time required for the heated layer to reach the boiling point. In order to do this we will assume that all the power provided by the laser beam is absorbed within the layer, thus neglecting any source of losses (reflection of the laser radiation in the donor system, lateral heat diffusion in the scanned line, etc.), and that the layer is uniformly heated. In this calculation we should first of all estimate the superheat required for bubbles to nucleate, since for a liquid film a few tens of microns thick the amount of superheat can be considerable. This estimation requires to postulate the dimensions of the nucleation sites, which obviously have to be much smaller than the thickness of the liquid film. Accordingly, we have assumed a radius (R) for the nucleation sites of about 1 μm, approximately halfway in order of magnitude between the thickness of the film and the dimensions of the Ag particles suspended in the ink. Therefore, the combination of Clausius-Clapeyron and Young-Laplace equations[4] provides an amount of superheat (ΔT_{SH}) of:

$$\Delta T_{SH} = \frac{2\gamma T_S}{L\rho_v R} \sim 20\ K \qquad (3)$$

where γ, L and ρ_v are respectively the surface tension, latent heat of vaporization and density of the vapor (in this case water, the main solvent of the ink; values provided in Table S1) and T_S the saturation temperature at room pressure (in this case 373 K). So, the temperature required for boiling inception (T_B) is 393 K.

The time required to initiate boiling of the heated layer is, therefore:

$$t_B = \frac{\pi \rho_m D^2 l_{th} c_p (T_B - T_o)}{4W} \sim 8\ \mu s \qquad (4)$$

where T_o corresponds to room temperature (300 K) and W to laser power (of the order of 1 W according to the experiments). The comparison of Eq. 5 with Eq. 1 ($t_B << t_i$) indicates that achieving the boiling temperature only takes a small fraction of the total irradiation time and that, therefore, boiling inception occurs during the early stages of the irradiation process.

As the final step in this discussion we should now estimate the time required for a bubble to nucleate (t_N). If we assume that this time will be of the same order than that corresponding to a cavitation bubble submitted to a tension equivalent to the difference between the vapor pressure of the liquid at T_B and room pressure, it can be calculated as:[4]

$$t_N \sim \frac{2\gamma}{\rho_L R} \frac{1}{\Sigma^2} \sim 1\ \mu s \qquad (5)$$

where ρ_L is the density of the liquid (water in this case; Table 1) and Σ is a function of different thermodynamic parameters of the liquid with a strong dependence on temperature;[4] at a T_B of 393 K it takes a value of around 10^4 m/s$^{3/2}$. In the same way as with t_B, in this case $t_N << t_i$, which indicates that many consecutive bubbles could nucleate during the entire irradiation time.

In summary, according to these estimations: 1) the entire ink volume scanned by the laser beam can be heated up to the boiling temperature of the solvent in a much shorter time than that during which the ink is irradiated, and 2) the total irradiation time is also much longer than that required for a bubble to nucleate, so that a large number of consecutive bubbles can be generated per unit volume in the ink. The burst of these bubbles once they reach the donor film surface would account for the spray observed during transfer. Therefore, the characteristic lengths and times of the process analyzed here indeed seem consistent with the hypothesis of pool boiling.

REFERENCES

(1) Vera-Agullo, J.; Varela-Rizo, H.; Conesa, J.A.; Almansa, C.; Merino, C.; Martin-Gullon, I. Evidence for Growth Mechanism and Helix-Spiral Cone Structure of Stacked-cup Carbon Nanofibers. *Carbon* **2007**, 45, 2751-2758.

(2) Breckenfeld, E.; Kim, H.; Auyeung, R. C.; Piqué, A. Laser-induced Forward Transfer of Ag Nanopaste. *J. Vis. Exp.* **2016**, 109, e53728, doi:10.3791/53728.

(3) Baker, M. How Quality Control Could Save Your Science: It May Not Be Sexy, but Quality Assurance Is Becoming a Crucial Part of Lab Life. *Nature* **2016**, 529, 456-458.

(4) Brennen, C.E. Cavitation and Bubble Dynamics. *Oxford University Press*, New York, **1995**.